Article:
Fulchini, F, Zafar, U, Hare, C et al. (4 more authors) (2017) Relationship between Surface Area Coverage of Flow-Aids and Flowability of Cohesive Particles. Powder Technology, 322. pp. 417-427. ISSN 0032-5910

https://doi.org/10.1016/j.powtec.2017.09.013

Accepted Manuscript

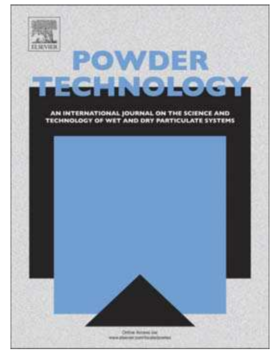

Relationship between surface area coverage of flow-aids and flowability of cohesive particles

Fabio Fulchini, Umair Zafar, Colin Hare, Mojtaba Ghadiri, Hossam Tantawy, Hossein Ahmadian, Massimo Poletto

PII: S0032-5910(17)30738-6
DOI: doi:10.1016/j.powtec.2017.09.013
Reference: PTEC 12818

To appear in: *Powder Technology*

Received date: 23 February 2017
Revised date: 8 August 2017
Accepted date: 6 September 2017

Please cite this article as: Fabio Fulchini, Umair Zafar, Colin Hare, Mojtaba Ghadiri, Hossam Tantawy, Hossein Ahmadian, Massimo Poletto, Relationship between surface area coverage of flow-aids and flowability of cohesive particles, *Powder Technology* (2017), doi:10.1016/j.powtec.2017.09.013

Relationship between Surface Area Coverage of Flow-Aids and Flowability of Cohesive Particles

Fabio Fulchini[1,3], Umair Zafar[1], Colin Hare[1§], Mojtaba Ghadiri[1*], Hossam Tantawy[2], Hossein Ahmadian[2], and Massimo Poletto[3]

[1]Institute of Particle Science and Engineering, School of Chemical and Process Engineering, University of Leeds, Leeds LS2 9JT, UK
[2]Procter and Gamble, Newcastle Innovation Centre, Longbenton, Newcastle upon Tyne, NE12 9TS, UK
[3]Department of Industrial Engineering, University of Salerno
[*]Corresponding Author Tel: +44 (0) 113 343 2406 , Email: m.ghadiri@leeds.ac.uk

Abstract

Poor and inconsistent flow of cohesive powders is a major issue in powder processing. A common solution is to coat the surfaces of the cohesive particles with finer particles, referred to as flow-aids. Such particles adhere to sticky surfaces and act as spacers preventing them from contacting each other and thus reducing the inter-particle forces and bulk powder cohesion. A question which naturally arises is how much flow-aid is needed to enhance the flowability to an optimum level. This work aims to establish a relationship between the degree of Surface Area Coverage (SAC) of flow-aids and the flowability, the latter as determined by a quasi-static shear cell method, as well as the angle of repose test and the FT4 powder rheometer. Glass beads of 90-150 μm sieve cut are made cohesive by silanising their surfaces with a commercial chemical reagent, Sigmacote® and are used as host particles. Two types of zeolite particles are used as flow aids. The mass fraction of the flow aids required to achieve a theoretical SAC of 1, 5, 10, 20, 50 and 100% is first estimated and then the host particles are coated in a pan mixer. The SAC is measured by Scanning Electron Microscopy, coupled with image analysis, and found to correlate well with the estimated value. The optimum surface coverage is found to be when SAC is 10-20%, as this provides the greatest flowability. An increase in SAC beyond this range leads to a gradual reduction in flowability.

---

§ Department of Chemical and Process Engineering, University of Surrey, Guildford, GU2 7XH, UK

(Keywords: cohesive, flowability, flow aids, processing, Surface are coverage, coating)

Nomenclature

GB	glass Beads	
SGB	silanised Glass Beads	
ZA	Zeolite A	
ZA-Ae	Zeolite A coated with 0.25% of nano-particles of aerosil	
D_{50}	50^{th} percentile of the cumulative particle size number distribution	μm
SAC	theoretical Surface Area Coverage	-
SAC_{actual}	actual Surface Area Coverage	-
ω	mass fraction of flow aids	-
N	number of guest particles on the surface of one host particle	-
A_G	sphere-equivalent projected area of one guest particle	m^2
S_H	sphere-equivalent surface area of one host particle	m^2
ρ_H	host particle density	kg/m^3
ρ_G	guest particle envelope density	kg/m^3
V_H	sphere-equivalent volume of one host particle	m^3
V_G	sphere-equivalent volume of one guest particle	m^3
ffc	flow function coefficient	-
θ	angle between the equatorial plane and the top of a sphere	rad
A_{Gi}'	area covered by guest particles in the i-th annular region	m^2
A_{ARi}	area of a i-th annular region	m^2
X_i	fraction of the i-th annular region covered by guest particles	-
A_{Gi}	area covered by guest particles in the i-th annular region corrected according to its position on the surface of the host particle	m^2

1. Introduction

Flowability and inter-particle forces are closely related. If particles have a weight much larger than the attractive inter-particle forces they may easily roll over one another, and as a consequence, they pack tightly and also flow easily [1]. When this is not the case, particles can attract each other, resulting in bulk cohesion, which is generally undesirable as it causes poor flow and arching [2]. Controlled cohesion is however desirable in instances such as mixing, as it mitigates the segregation [3], and drug release in dry powder inhalers [4]. The smaller the size of the particles, the stronger the inter particle interactions become, such as van der Waals, capillary and electrostatic forces with respect to particle weight. Inter-particle forces depend on the local radius of curvature at contact [5]. The strength of such forces can be decreased by decreasing the local asperity radius, as irregularly-shaped fine particles flow better than round particles [1]. For this reason particles are often coated with hard very fine particles, called flow control additives, or flow aids, in order to separate energetic surfaces and to decrease the local radius of curvature at contact, thus reducing van der Waals interactions down to several orders of magnitude [5]. Inter-particle force reduction therefore results in improvement of bulk properties, such as flowability, bulk density [6], and fluidisation behaviour [7]. In industry it has become a common practice to coat the host particles with small and hard nano-particles, referred to as guests as shown schematically in Figure 1.

Figure 1. Schematic illustration of the coating mechanism

Guest particles act as spacers among host particles, increasing the separation distance and therefore reducing the intensity of van der Waals attraction between host particles [8]. Van der Waals forces obviously also prevail in contacts between host and guest particles, ensuring that guests remain on the surfaces of the host particle as their weight is much smaller than the attractive forces. As a result, simple physical surface modifications, such as coating by fine particles, can lead to improvements in flow properties and poured bulk density of powders. Of course, understanding the effect of the surface area coverage of host particles by flow additives on the flowability of the bulk is helpful to optimise the coating process. For example, Conesa *et al.* [9] show that coating the surfaces of polyester-based particles with a layer of silica nano-particles, at 0.3 wt%, leads to an optimum flowability. They propose that for higher amounts of the guest particles, the host-guest contacts are replaced with guest-guest contacts, and this change is responsible for the decrease of the powder flowability. Castellanos [1] calculates this critical value of the surface area coverage (SAC), assuming that both host and guest particles are spherical and the latter is uniformly distributed on the surfaces of the former, where the mass fraction of flow aids is defined as the ratio of mass of guest particles over the mass of host particles. He shows that this transitional SAC value is independent of size and density and is equal to $\pi/16\times100$, which is roughly 20%. In an earlier work, Chen *et al.* [10] showed that in order to have guest-guest particle contacts whenever two coated particles come in contact, SAC should be between 20% and 100%. Yang *et al.* [11], using cornstarch powder of 15 μm mean diameter as host particles and five types of nano-sized guest particles, demonstrate that the flow improvement is not directly related to the mass of flow aids used, but rather to the obtained SAC; different coating techniques give rise to different levels of SAC. They use four different techniques including hand mixing, a Hybridizer (equipment generating high impaction forces), a V-Blender and a Magnetic Assisted Impaction Coating (MAIC) device. Using the MAIC technique, they obtained the best match of theoretical and actual SAC, as well as the best flowability improvement. Jallo *et al.* [12] coat different combinations of API powders, using nano-silica particles as flow aids at 1 wt% by MAIC, resulting in different SAC values ranging between 46.2% and 1068%, the latter implying either multilayer coating or loose flow-aids particles in the interstices of the host particles. They obtain the best flow function coefficient (ffc) for a theoretical SAC of 293%. Zhou *et al.* [13] coat particles of α-lactose monohydrate, of 20 μm median particle size, with nano-particles of magnesium stearate (MgSt) powder by mechanofusion at 0.1, 0.5, 1, 2, 5 wt% loading. They find major improvements in flowability as measured by the shear cell at 0.5 wt% of flow aids or higher. They evaluate the surface coverage as the normalised Mg counts over the total counts for all species by X-Ray photoelectron spectroscopy (XPS) and Time-of-flight of the secondary ion mass spectrometry (Tof-SIMS). For the 0.5 wt% sample the coverage was estimated to be 64.5%.

The addition of a known mass of flow aids does not necessarily gets fully dispersed on the surfaces of the sticky particles. Therefore the aim of the present work is to establish a direct relationship between SAC and flowability. For this purpose, glass beads are made cohesive by a silanisation process and are used as host particles, while two types of zeolite particles are used as guest particles. Coating is carried out in a rotary pan coater. The theoretical SAC is defined as the percentage of surface area of the host particles that is covered by the projected area of the guest particles. SAC is varied from 1 to 100%. The coating uniformity is checked by Scanning Electron Microscope (SEM) and the micro-graphs are used to calculate the actual SAC by the image analysis method. The flowability of the samples is then evaluated using three different techniques: Schulze annular shear cell, angle of repose and the Freeman FT4 powder rheometer.

2. Materials and Method

2.1. Materials

The host particles are 90-150 μm glass beads made cohesive by silanisation with Sigmacote®. Two different flow aid particles are used, namely Zeolite A (ZA), as shown in Figure 2, and Zeolite A coated with 0.25 wt% of nanoparticles of Aerosil (ZA-Ae). These are referred to as guest particles. The maximum projected area equivalent circle diameter is measured for both guest and host particles by Malvern Morphologi G3. The number distribution of particle size for all the materials is then obtained. The 50th percentile of the cumulative distribution (D_{50}) is reported in Table 1, as well as the particle shape and envelope density.

Table 1. Host and Guest Particle properties

Figure 2. Zeolite A particles

Bulk cohesion and density of the glass beads before and after silanisation and of the flow aids themselves have been evaluated by a Schulze RST-XS shear cell, and are reported in Figure 3.

Figure 3. Bulk density and cohesion as affected by silanisation of glass beads and coating of zeolite particles by Aerosil

The silanisation process has increased the bulk cohesion of the glass beads and, as a direct consequence, bulk density is reduced. Both ZA and ZA-Ae present a very high cohesiveness. It is also notable how the use of Aerosil nano-particles could reduce the cohesion of ZA as well as increase its bulk density.

2.2. Method

2.2.1. Calculation of the theoretical SAC

In order to obtain a surface area coverage of 1, 5, 10, 20, 50, 100%, the required amount of flow aids is calculated according to eq. 1-3, making the assumptions: (i) both host and guest particles are spherical and are sized equal to their D_{50}; (ii) the covered surface area of the host is equal to the total projected area of the guest particles; (iii) the guest particles form a monolayer on the surface of the host particles; (iv) the host and guest particles are fully mixed and the host particles are uniformly coated.

We define the mass fraction of guest particles, ω, as the ratio of the mass of guest particles on one host particle over the total mass of the host and guest particles:

$$\omega = \frac{N\rho_G V_G}{N\rho_G V_G + \rho_H V_H} \times 100 \tag{1}$$

whereas N is the number of guest particles on the surface of one host particle, ρ_H, V_H, ρ_G, V_G are the particle density and volume of host and guest particles, respectively. This definition differs from that used by Castellanos [1], who used only the mass of the host particle in the denominator. Nevertheless, the difference is negligible as the mass of the guest particles constitutes a very small fraction of the whole mass.

The SAC is defined as the degree of coverage of the host particle surface area by the guest particles:

$$SAC = \frac{NA_G}{S_H} \tag{2}$$

where A_G is the projected area of one guest particle and S_H is the surface area of one host particle. We use eq. 2 to get N and use the result in eq. 1, to get ω as a function of SAC, eq. 3:

$$\omega = \frac{S_H\rho_G V_G SAC}{S_H\rho_G V_G SAC + A_G\rho_H V_H} \times 100 \tag{3}$$

The values of ω calculated from eq. 3 for the host and guest particles considered here for 1, 5, 10, 20, 50 and 100% SAC are reported in Table 2. The mass percentages for both ZA and ZA-Ae are the same as the presence of aerosil is not taken into account.

Table 2. Mass fractions of flow aids for the set surface area coverages (SAC)

2.2.2. Coating Process

The coating process was performed using a pan mixer of 0.4 m diameter, inclined at an angle of 45° with respect to the horizontal axes. Each sample of 150 g of host particles is first added to the pan, then guest particles are manually added gradually along 35 minutes at a constant rotational speed of 100 rpm.

2.3. Image analysis and actual SAC

Coated particles are viewed by Scanning Electron Microscopy (SEM). The micrographs are used to assess the quality of coating in terms of guest particle dispersion on the surfaces of the host particles and also to calculate the actual SAC achieved by image analysis using ImageJ. The SEM micrographs are converted to binary images so that guest particles can be distinguished from the rest, as shown in Figure 4.

Figure 4. Micrographs and image manipulation for SAC evaluation

Due to the spherical shape of the host particles, the measured projected area should be converted to the real area. The required correction increases as the diametral plane is approached, as it is schematically represented in Figures 5a and 5c. The projection correction is proportional to $1/\sin\theta_i$, where θ_i is the angle between the equatorial plane and the position on the surface as shown in Figure 5b. The top view of the particle is divided into "n" annular concentric regions as shown in Figure 6. For each annular region its median radial distance from the centre, r_i, is determined, where "*i*" is the index of the annular region, as indicated in Figure 5. For every annular region, the ratio between the number of black pixels over the total number of pixels, X_i, as obtained from image analysis, is equal to the ratio of the two areas in the *i*-th annular region, i.e. the black area, A_{Gi}', and the total projected area, A_{ARi}.

$$X_i = \frac{A_{Gi}'}{A_{ARi}} \tag{4}$$

A_{Gi}' is then corrected accordingly due to its position on the hemisphere to give the actual black area, A_{Gi} :

$$A_{Gi} = \frac{A_{Gi}'}{\sin\theta_i} \tag{5}$$

It is noteworthy that at the very periphery of the surface the calculation of the coverage could be overestimated due to the contribution given by the lateral area of the guest particles (proportional to the thickness of the layer) to A_{Gi}', as shown in Figure 7. To avoid this effect, although small, the analysis is limited to a smaller portion of the particle so the SAC is defined according to eq. 7. In general, the very peripheral area of the host particle is not considered, i.e. the last annular ring.

$$SAC_{actual} = \frac{\sum_{i=1}^{n} A_{Gi}}{\frac{S_H}{2}\left[1-\cos(\theta_n)\right]} \tag{7}$$

Figure 5. Schematic representation of a coated particle: a) 3D view of half coated particle; b) hemisphere section; c) top view of the hemisphere

Figure 6. Annular divisions of the particle top view

Figure 7. A guest particle and its binary corresponding positioned at the top (a) and at the periphery of the host particle (b)

2.4. Flowability assessment

2.4.1. Shear Cell

Shear cell measurements are taken using a Schulze RST-XS ring shear tester (Wolfenbüttel, Germany) at pre-consolidation loads of 3, 5 and 10 kPa to determine the flow function coefficient (ffc). According to the classification of Jenike [14], the ffc is defined as the ratio of the pre-consolidation major principal stress, σ_1, and the unconfined yield stress, σ_C. ffc describes the ease with which material flow is initiated as shown in Table 3.

Table 3. Flow function coefficient (ffc) classification according to Jenike [13]

2.4.2. FT4

In the FT4 Powder Rheometer (Freeman Technology, Tewkesbury, UK), the flow behaviour of bulk solids is evaluated by considering the total energy (work) dissipated by a rotating impeller blade driven through a column of powder [15]. The powder is first brought to a reproducible packing state by the impeller blade rotating clockwise, descending and ascending through the bed, thereby cutting and lifting it to establish a consistent and reproducible packing density. Following this stage, the blade then moves downward, whilst rotating anticlockwise, thereby pressing down and shearing the powder bed. The expended work is measured and termed the total flow energy. The test procedure is such that the bed volume is kept constant, and therefore if the packing density changes between tests, as is the case here due to the addition of flow-aids, it is more appropriate to express the expended work per unit bed mass. It is also possible to measure the expended work associated with the blade whilst driven upwards through the bed and rotating anticlockwise, but this mode was not addressed in this work. The experiments here were carried out using a constant blade speed of 10 mm/s, and the average of 10 repeats is reported.

2.4.3. Angle of Repose (AoR)

The angle of repose is evaluated following the procedure and the equipment of Geldart [16].

Table 4. Classification of the Angle of Repose (AoR) according to Carr [17] and Raymus [18]

3. Results and Discussion

3.1. SEM analysis and Actual Surface Area Coverage

Figures 8 and 9 show SEM micrographs of silanised glass particles coated at different degrees of SAC with ZA and ZA-Ae, respectively. Inspection of the figures indicates that the guest particles are in general well dispersed on the surfaces of the host particles. Given the higher cohesiveness of ZA than ZA-Ae, the formation of little clusters of guest particles at high degrees of coverage is observed, especially at 100% of SAC as shown in Figure 8. In contrast, in the case of ZA-Ae, the guest particles seem to be much better dispersed on the host particle surface and to individually contact the surface. This difference in dispersion would affect the effectiveness of the flow aid to improve the powder flowability. Nevertheless, the actual SAC measured according to eq. 7 corresponds well to the theoretical values, as reported in Table 5. It is also interesting to note that for doublets, the guest particles accumulate in the valleys, presumably due to less prevailing shear stresses therein. It implies that for non-spherical host particles ridges are likely to be covered with the guest particles first.

Figure 8. SEM micrographs of particles coated with ZA, from top left to bottom right: 1, 5, 10, 20, 50, 100% of SAC

Figure 9. SEM micrographs of particles coated with ZA-Ae, from top left to bottom right: 1, 5, 10, 20, 50, 100% of SAC

Table 5. Theoretical and actual SAC

3.2.Flowability Measurements

3.2.1. Shear Cell

The flow function of silanised glass particle coated at different degrees of SAC with ZA and ZA-Ae is obtained at three applied normal stress as shown in Figures 10 and 11, respectively. For silanised glass particles coated with ZA, Figure 10 indicates that the flowability improves as the degree of coverage reaches around 20%, after which it reduces to a value as low as SAC 0% (i.e. uncoated silanised glass beads) for SAC 50% and 100%. It is noteworthy that in the case of SAC of 50% or 100% the application of 10 kPa pre-consolidation load results in less flowable material then the uncoated silanised glass beads. The same behaviour is found for the silanised glass beads coated with ZA-Ae, as shown in Figure 11.

Figure 10. ffc of SGB coated with ZA

Figure 11. ffc of SGB coated with ZA-Ae

It is clear from the shear cell results that the best flowability is obtained for an SAC of 10-20%. A full coverage leads to poor flowability. A comparison of the extent of improvement for the 20% of SAC and reduction for the 100% of SAC between the two flow aids is reported below in Table 6. The ffc change is calculated as

$$\frac{ffc_{20\%} - ffc_{0\%}}{ffc_{20\%}} \tag{8}$$

at 20% SAC and:

$$\frac{ffc_{100\%} - ffc_{0\%}}{ffc_{0\%}} \tag{9}$$

at 100% SAC. Of course, positive value correspond to an improvement of flowability, while negative values to a worsening. ZA shows larger improvements in flowability than ZA-Ae at 20% of SAC, and also less worsening in the case of full coverage. A possible explanation of this difference can be related to the quality of dispersion achieved in the coating processes, being less uniform for ZA. These particles are in fact present in little clusters rather than individuals, in contrast to ZA-Ae as shown in Figures 8 and 9. Consequently, the actual SAC of ZA is in fact further from the theoretical value, Table 5, but the flowability is improved to a greater extent because the little clusters act as bigger spacers compared to individual particles. A more systematic study of the effect of the guest particle size is therefore of interest.

Table 6. Changes of ffc at 20% and 100% of SAC for the two flow aids (positive values correspond to an improvement of flowability, while negative values to a worsening)

3.2.2. Flowability Indicator by Flow Energy Measurement by FT4

The outcomes of the FT4 measurements are reported in Figure 12 in terms of the total flow energy per unit bed mass, a larger value indicating a greater resistance to shearing the bed due to bulk cohesion. The best flowability, associated with the lowest expended work, is found again for an SAC of 20%. Moreover, ZA improves the flowability of cohesive beads more than does ZA-Ae.

Figure 12. Total flow energy per unit bed mass of SGB coated with ZA and ZA-Ae at different SAC

3.2.3. Angle of Repose

Photographs of the repose angles are shown in Figure 13 for different degrees of coverage, where the change in the repose angle is clearly visible. The pile of powder becomes flatter (index of good mobility of particles) as the SAC is increased to 20%. Apart from the height of the pile, another good indication of particle mobility, and therefore flowability, is given by the base of the piles, being faint or well defined for more and less cohesive particles, respectively, reflecting the spreading of the former. The results of the measured repose angle measurements are shown in Figure 14. Remarkably, the results confirm the outcomes of the shear cell and the FT4 measurements. The best flowability is again found at 20% of SAC, it almost reaches the angle of repose of the glass beads with no silanisation. In line with the other two measurements methods, as the SAC is increased to 50 and 100% cohesiveness is slightly increased, indicated by AoR increasing again to around 32° at SAC 100%.

Figure 13. AoR of SGB, SGB+ZA-Ae at increasing SAC and GB, respectively

Figure 14. Angle of Repose of Silanised Glass Beads (SGB) coated with ZA-Ae at different SAC

3.3. Discussion

All the flowability test methods are remarkably consistent in revealing that flowability improves as the SAC is increased up to 20% and then it deteriorates beyond this, for both cases of flow aids, i.e. ZA and ZA-Ae. This critical value is therefore the SAC for which the host-host particle contact is minimized. The higher effectiveness of the ZA flow aid as compared to that of the ZA-Ae, indicates agglomerated guest particles can be more effective than a perfect monolayer of the guest particles, suggesting that the size of the guest particles plays a role by increasing the separation distance between sticky surfaces. A systematic study of the effect of the guest particle size acting as a spacer will therefore be of great interest. Furthermore, the zeolite particles used here are cuboidal shape, as shown in Figure 2, and the presence of edges and corners may in fact be beneficial to reducing adhesion, in contrast to spherical guest particles. This feature is also worthy of investigation, although the choice of flow aids is very limited. Magnesium stearate is commonly used as lubricant, as it readily delaminates on shearing exposing low-energy low-frictional cleavage planes [19]. However, its presence in fine particulate form provides a similar "spacer" effect to reduce host inter-particle stickiness. Above the optimum critical value of the guest particle loading, the number of effective contacts between guest-guest particles coming from different host particles per unit volume increases. This leads to a deterioration in flowability. This finding is more pronounced in the case of good dispersion of the flow aid with ZA-Ae at high degrees of coverages like 50% and 100%. From the above it appears, therefore, that an important parameter is the cohesiveness of the flow aid itself, which affects the quality of coating and the flowability as a direct consequence. Particle shape has a strong influence on flowability. Addition of flow aids will initially lead to accumulation of flow aids in the concave regions of the surface as shown in Figure 9. Therefore larger quantities of flow aids will be needed to achieve similar flowability. The uniformity of the guest particles on the host particles surfaces could be influential, but is difficult to control, and more so for irregular host particle shapes.

4. Conclusions

The effect of the surface area coverage (SAC) on flowability of 90-150 μm glass beads, made cohesive by silanisation, has been assessed using two types of micrometre sized particles: Zeolite A (ZA) and Zeolite A coated with nano-particles of Aerosil (ZA-Ae). The particles are practically the same material, the only main difference lies in their cohesiveness; ZA-Ae being less cohesive than ZA. These flow aids act as spacers between cohesive surfaces, thus promoting flow despite being cohesive themselves. Silanised glass beads (SGB) are coated in a pan mixer at different theoretical SAC values of 1, 5, 10, 20, 50 and 100% of flow aids. The quality of coating is assessed by viewing the SEM micrographs of such samples. Moreover, the actual SAC is evaluated by image analysis and found to agree with the theoretical values. Flowability is assessed using the annular shear cell, FT4 powder rheometer and angle of repose measurements. The results from the three test methods are in remarkable agreement, and indicate an optimum flowability for a theoretical coverage of around 20%. Beyond this point the flowability decreases, though less dramatically for the SGB+ZA. The greater cohesiveness of ZA leads to their particles forming small clusters on the surfaces of the host particles, enhancing their spacer effect. This is not the case for ZA-Ae, as the particles are almost fully spread on the surfaces. The transition from host-guest particle contact to guest-guest particle contact is critical in terms of flowability, as the guest particles are cohesive themselves.

5. Acknowledgements

This article is dedicated to the memory of the late Professor Antonio Castellanos Mata, Universidad de Sevilla, Spain, whose pioneering work on the use of flow aids inspired this work.

The first author visited the University of Leeds on an Erasmus Exchange Programme with the University of Salerno in 2015 during which this work was carried out with partial support from Procter and Gamble Newcastle Innovation Centre, Newcastle upon Tyne, UK. The second author, U. Zafar, was supported by a Knowledge Transfer Secondment from the Impact Accelerated Award to the University of Leeds by the Engineering and Physical Sciences Research Council, UK (grant no. EP/K503836/1), working at Procter & Gamble Newcastle Innovation Centre, Longbenton, Newcastle upon Tyne, UK.

6. References

[1] A. Castellanos, The relationship between attractive interparticle forces and bulk behaviour in dry and uncharged fine powders, Adv. Phys. 54 (2005) 263–376.

[2] J.K. Prescott, R.A. Barnum, On Powder Flowability, Pharm. Technol. (2000) 60–84.

[3] C.F. Harwood, Powder Segregation Due to Vibration, Powder Technol. (1977) 51–57.

[4] M. Lohrmann, M. Kappl, H.-J. Butt, N.A. Urbanetz, B.C. Lippold, Adhesion forces in interactive mixtures for dry powder inhalers – Evaluation of a new measuring method, Eur. J. Pharm. Biopharm. (2007) 579–586.

[5] L. Massimllla, G. Donsi, Cohesive Forces Between Particles of Fluid-Bed Catalysts, Powder Technol. 15 (1956) 253–260.

[6] A.A. Kyrre Thalberg, David Lindholm, Comparison of different flowability tests for powders for inhalation, Powder Technol. 146 (2004) 206–213.

[7] J.M. Valverde, A. Castellanos, Types of gas fluidization of cohesive granular materials, Phys. Rev. E - Stat. Nonlinear, Soft Matter Phys. 75 (2007) 1–6.

[8] M.P. Mullarney, L.E. Beach, R.N. Dave, B.A. Langdon, M. Polizzi, D.O. Blackwood, Applying dry powder coatings to pharmaceutical powders using a comil for improving powder flow and bulk density, Powder Technol. 212 (2011) 397–402.

[9] C. Conesa, K. Saleh, A. Thomas, P. Guigon, N. Guillot, Characterization of Flow Properties of Powder Coatings Used in the Automotive Industr y †, Methods. 22 (2004) 94–106.

[10] Y. Chen, J. Yang, R.N. Dave, R. Pfeffer, Fluidization of Coated Group C

Powders, AIChE J. 54 (2008) 104–121.

[11] J. Yang, A. Sliva, A. Banerjee, R.N. Dave, R. Pfeffer, Dry particle coating for improving the flowability of cohesive powders, Powder Technol. 158 (2005) 21–33.

[12] L.J. Jallo, C. Ghoroi, L. Gurumurthy, U. Patel, R.N. Davé, Improvement of flow and bulk density of pharmaceutical powders using surface modification, Int. J. Pharm. 423 (2012) 213–225.

[13] Q. Zhou, L. Qu, T. Gengenbach, J.A. Denman, I. Larson, P.J. Stewart, D.A. V Morton, Investigation of the extent of surface coating via mechanofusion with varying additive levels and the influences on bulk powder flow properties, Int. J. Pharm. 413 (2011) 36–43.

[14] A.W. Jenike, Gravity Flow of bulk solids, Bull. Univ. Utah. 52 (1961) 24–27.

[15] R. Freeman, The classifications of powder in relation to flowability, Powder Handl. Process. 12 (2000) 194–197.

[16] D. Geldart, E.C. Abdullah, A. Hassanpour, L.C. Nwoke, I. Wouters, Characterization of powder flowability using measurement of angle of repose, China Particuology. 4 (2006) 104–107.

[17] R.L. Carr, Classifying flow properties of solids, Chem. Eng. 72 (1965) 69–72.

[18] G.J. Raymus, Handling of Bulk Solids, in: D. Green R. H. Perry (Ed.), Chem. Eng. Handb., 6th ed., McGraw Hill, New York, 1985.

[19] A. Mehrotra, M. Llusa, A. Faqih, M. Levin, F.J. Muzzio, Influence of shear intensity and total shear on properties of blends and tablets of lactose and cellulose lubricated with magnesium stearate, Int. J. Pharm. 336 (2007) 284–291.

Table 1. Host and Guest Particle properties

Role	*Material*	*Abbreviation*	*D_{50} [μm]*	*Shape*	*Density [kg/m³]*
Host Particles	Glass Beads made cohesive by silanisation	SGB	125	Spherical	2500
Guest Particles	Zeolite A	ZA	2.6	Cubical	1417
Guest Particles	Zeolite A (coated with nano particles of Aerosil)	ZA-Ae	2.6	Cubical	1417

Table 2. Mass fractions of flow aids for the set surface area coverages (SAC)

SAC [%]	1	5	10	20	50	100
ω [%]	0.05	0.24	0.47	0.94	2.32	4.53

Table 3. Flow function coefficient (ffc) classification according to Jenike [13]

ffc<1	Hardened
1<ffc<2	Very Cohesive
2<ffc<4	Cohesive
4<ffc<10	Easy Flowing
ffc>10	Free Flowing

Table 4. Classification of the Angle of Repose (AoR) according to Carr [17] and Raymus [18]

AoR>55°	Very High Cohesiveness
45°<AoR<55°	High Cohesiveness
30°<AoR<45°	Some Cohesiveness
AoR<30°	Good Flowability

Table 5. Theoretical and actual SAC

Theoretical SAC [%]	*1*	*5*	*10*	*20*	*50*	*100*
Actual SAC (SGB+ZA) [%]	0.7	3.5	5.5	20.0	41.2	66.9
Actual SAC (SGB+ZA-Ae) [%]	0.4	5.3	8.7	17.3	57.3	75.1

Table 6. Changes of ffc at 20% and 100% of SAC for the two flow aids (positive values correspond to an improvement of flowability, while negative values to a worsening)

	ffc change	
Flow aid	*20% SAC*	*100% SAC*
ZA	33.3%	-3.2%
ZA-Ae	21.3%	-23.1%

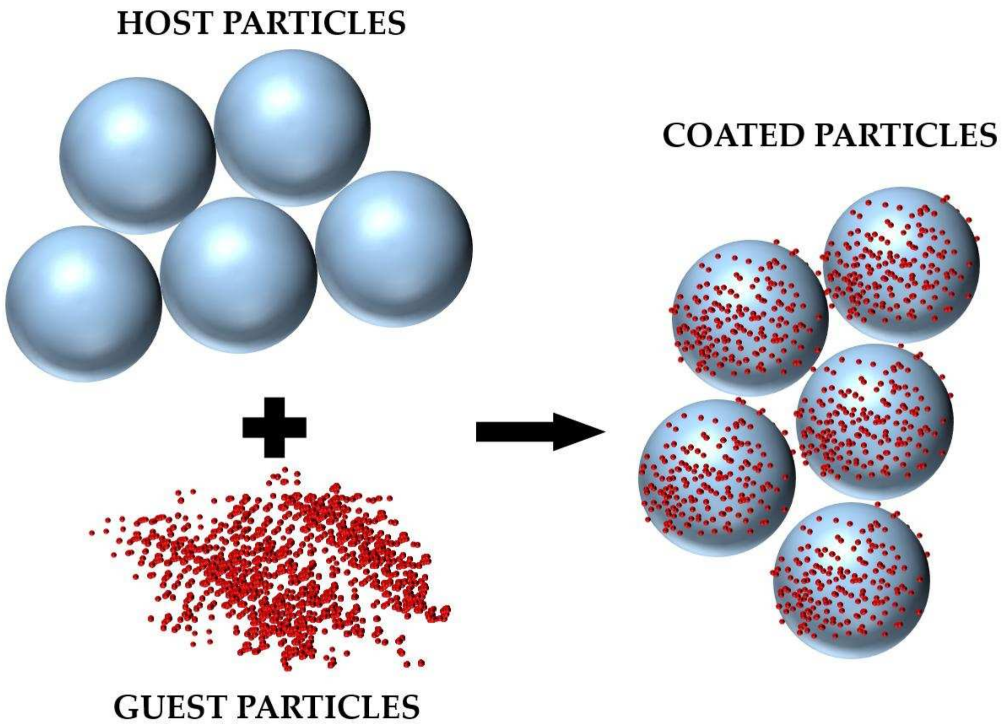

Figure 1. Schematic illustration of the coating mechanism

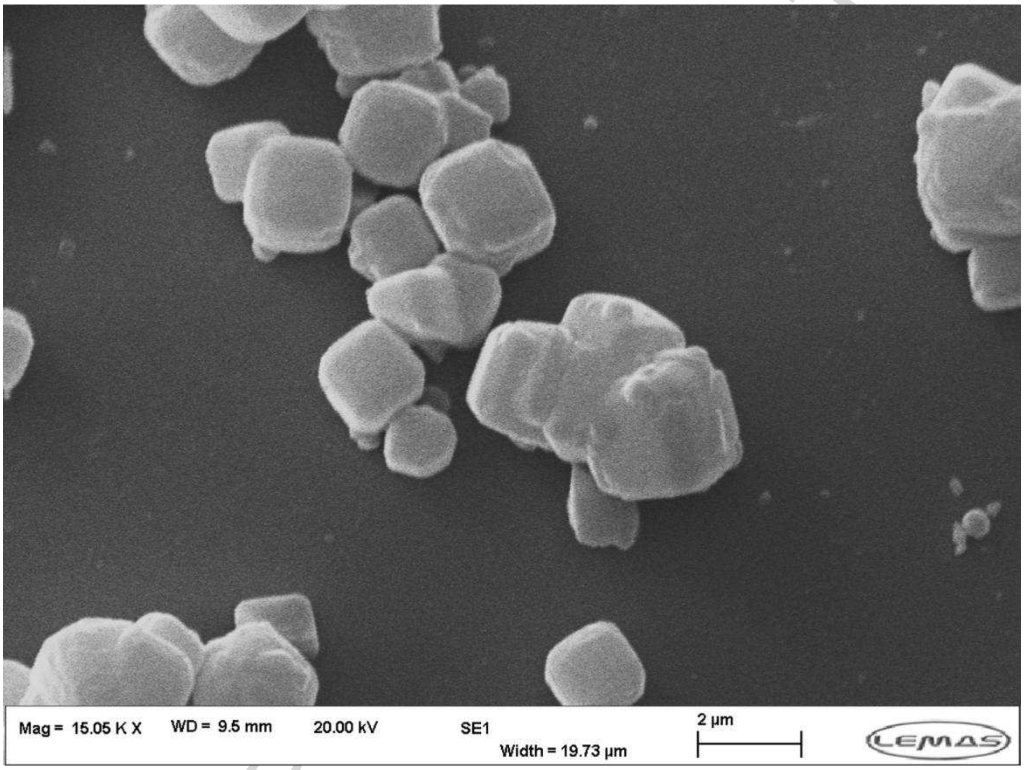

Figure 2. Zeolite A particles

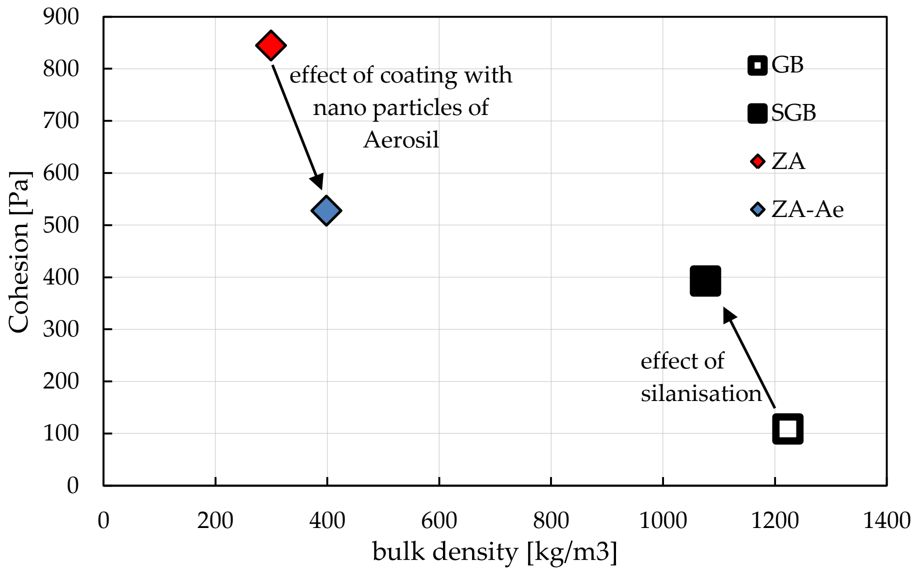

Figure 3. Bulk density and cohesion as affected by silanisation of glass beads and coating of zeolite particles by Aerosil

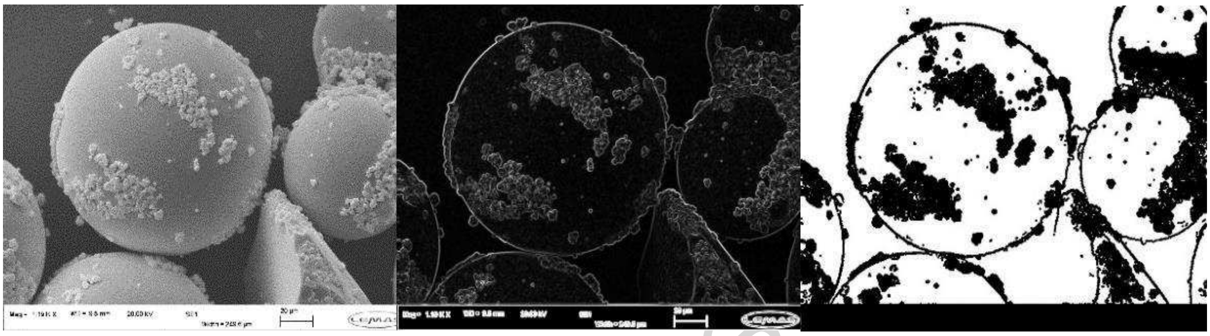

Figure 4. Micrographs and image manipulation for SAC evaluation

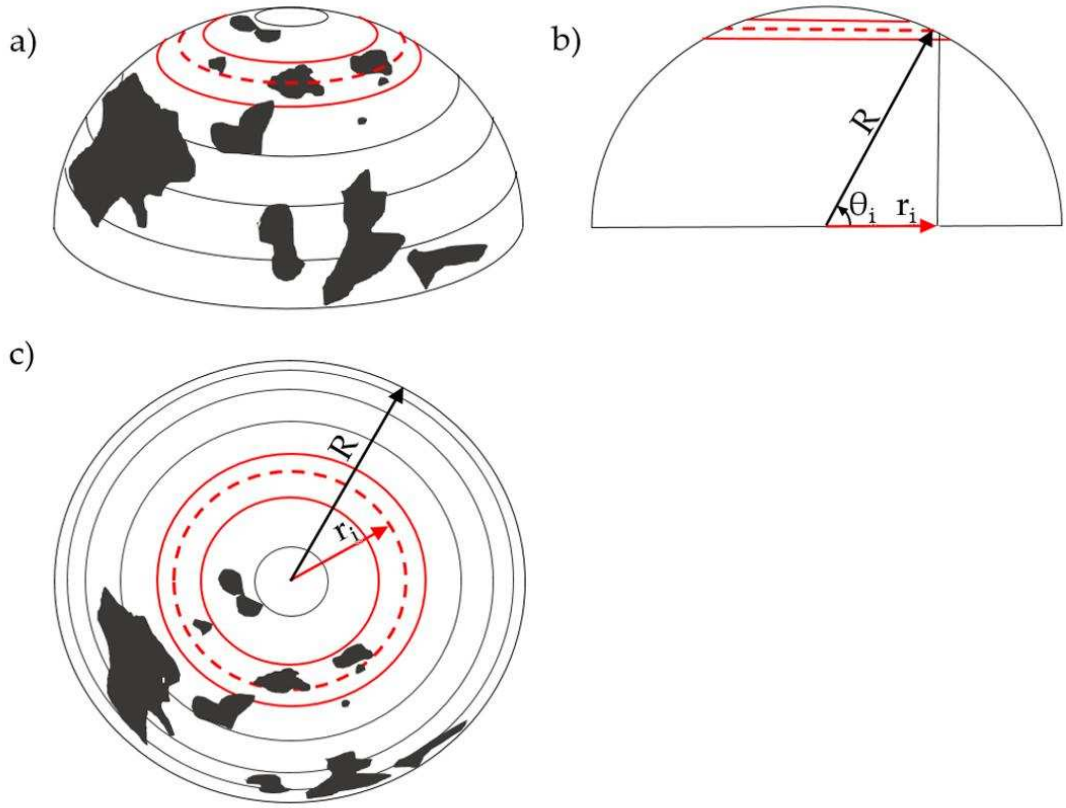

Figure 5. Schematic representation of a coated particle: a) 3D view of half coated particle; b) hemisphere section; c) top view of the hemisphere

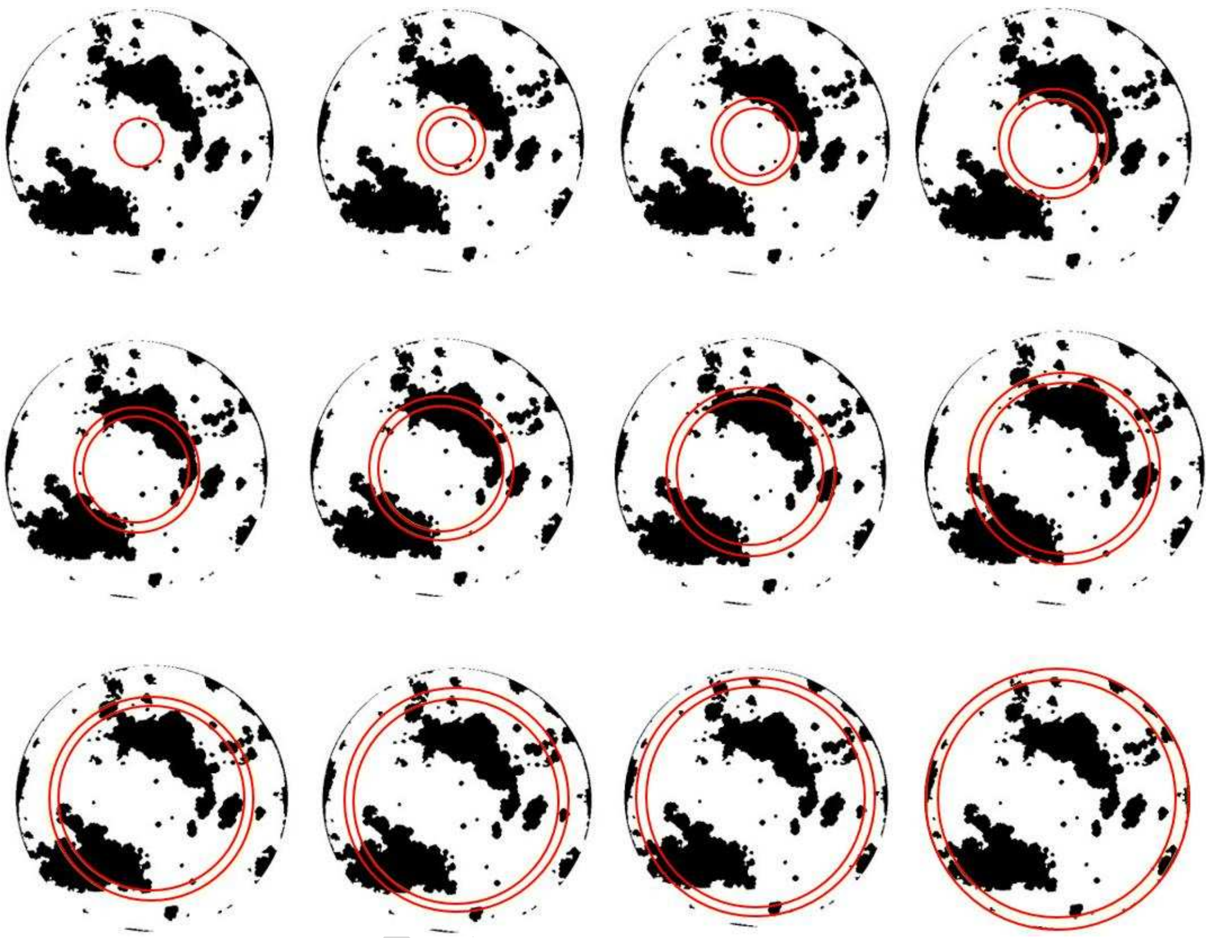

Figure 6. Annular divisions of the particle top view

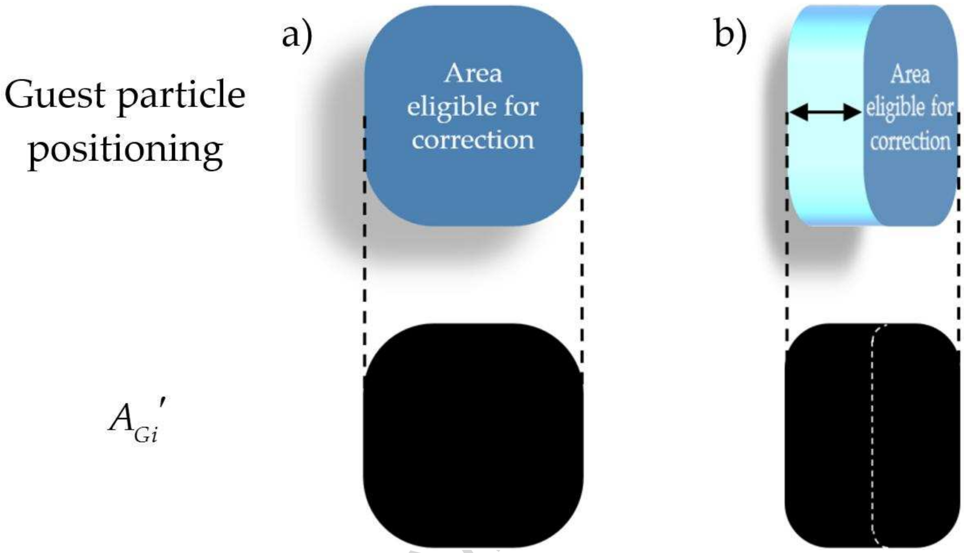

Figure 7. A guest particle and its binary corresponding positioned at the top (a) and at the periphery of the host particle (b)

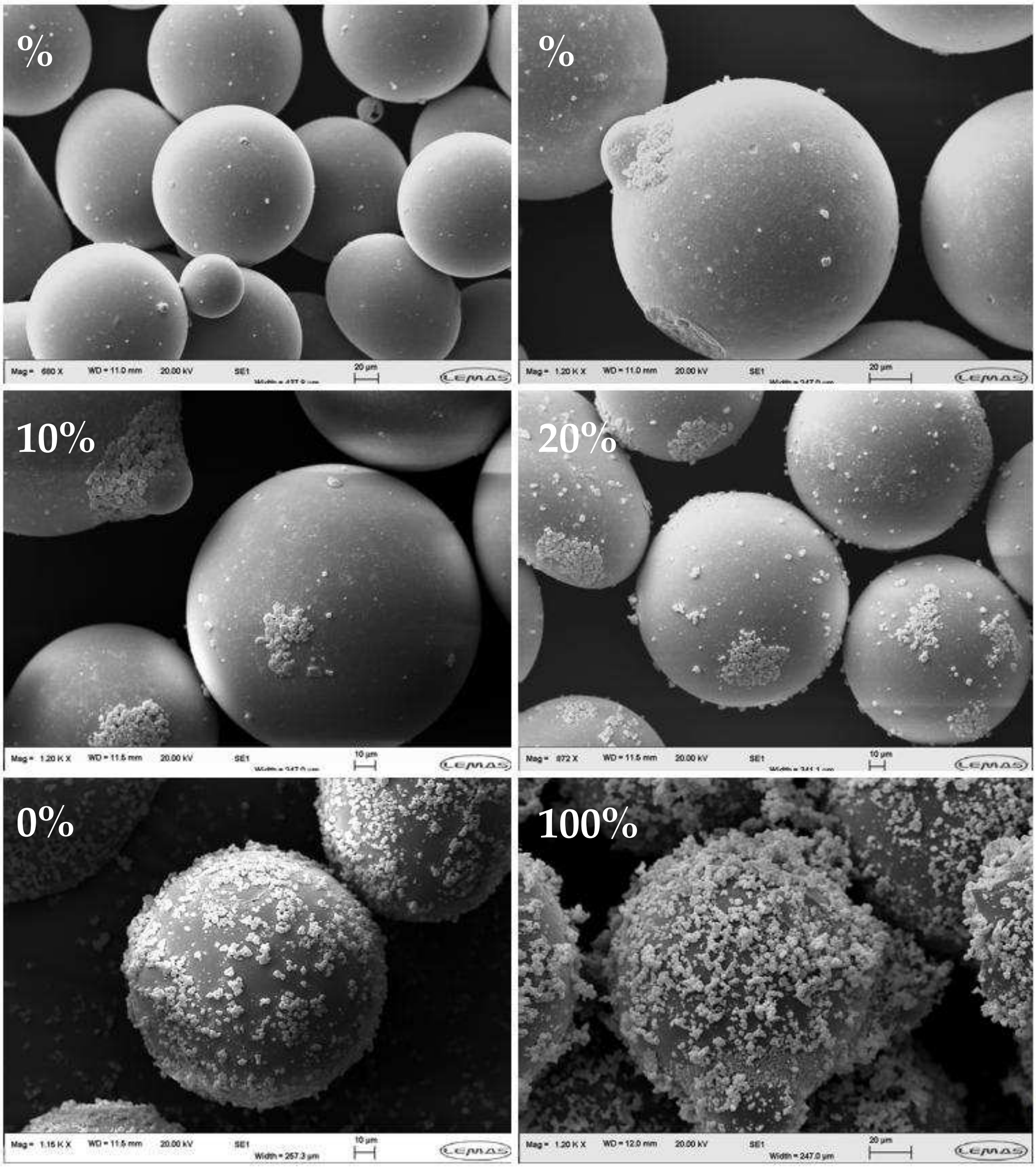

Figure 8. SEM micrographs of particles coated with ZA, from top left to bottom right: 1, 5, 10, 20, 50, 100% of SAC

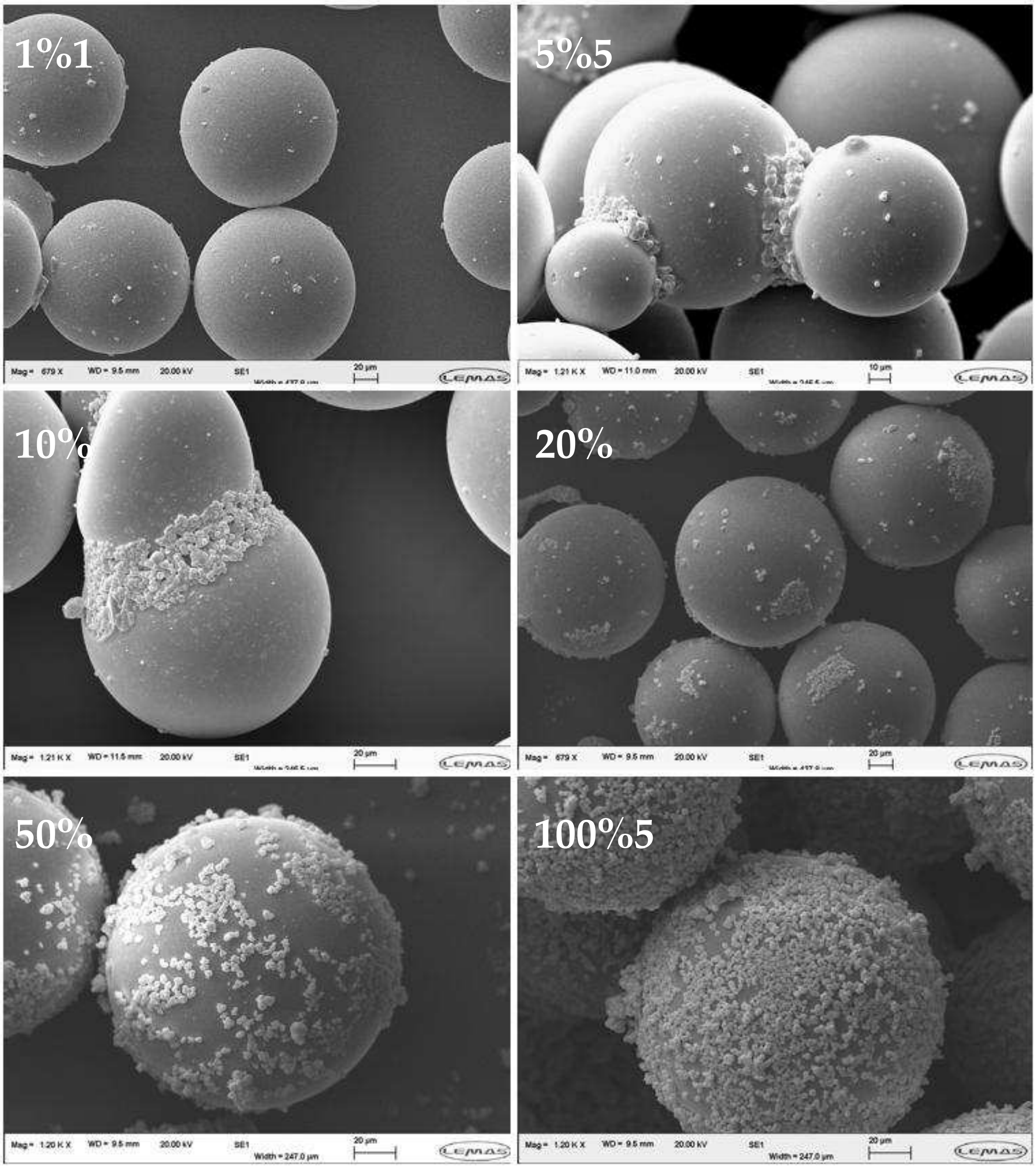

Figure 9. SEM micrographs of particles coated with ZA-Ae, from top left to bottom right: 1, 5, 10, 20, 50, 100% of SAC

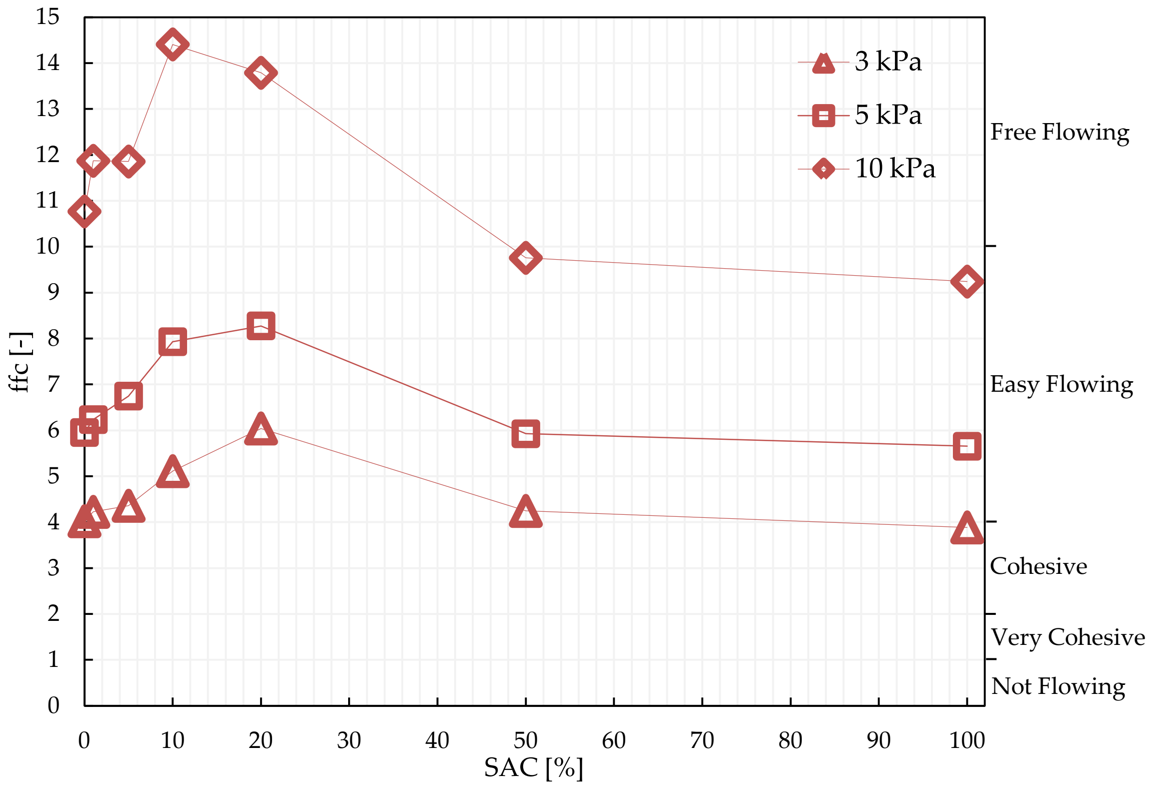

Figure 10. ffc of SGB coated with ZA

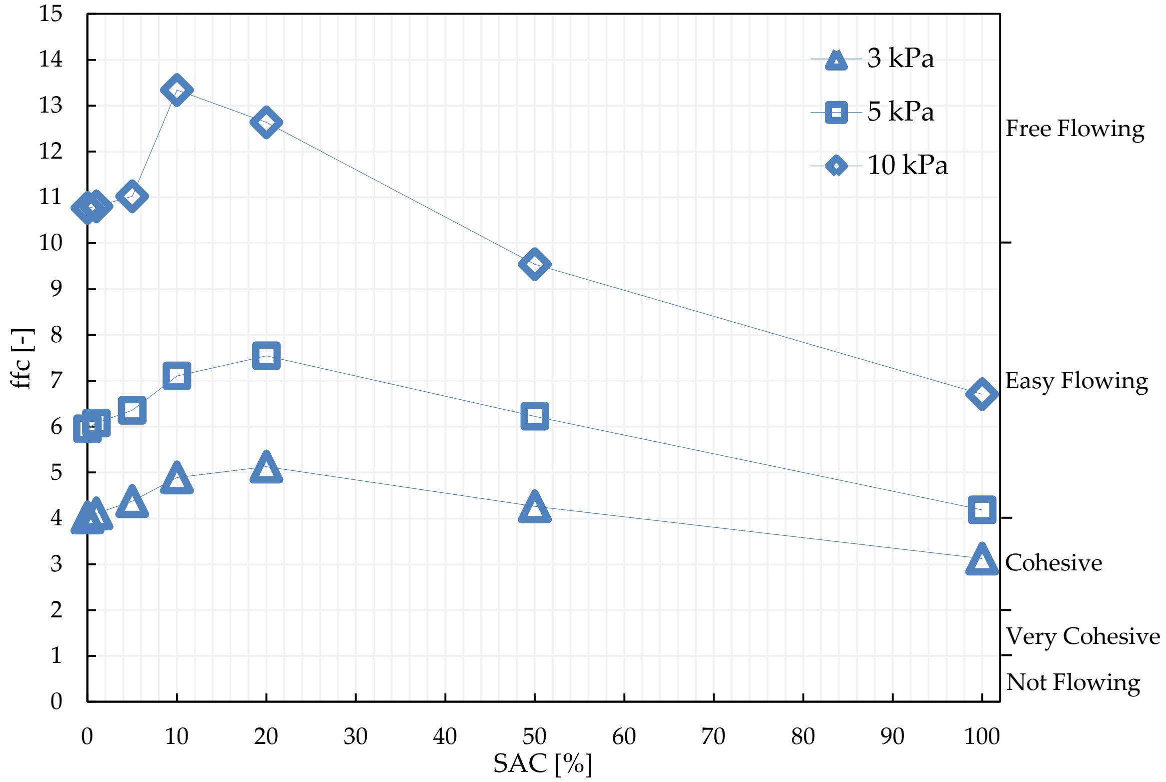

Figure 11. ffc of SGB coated with ZA-Ae

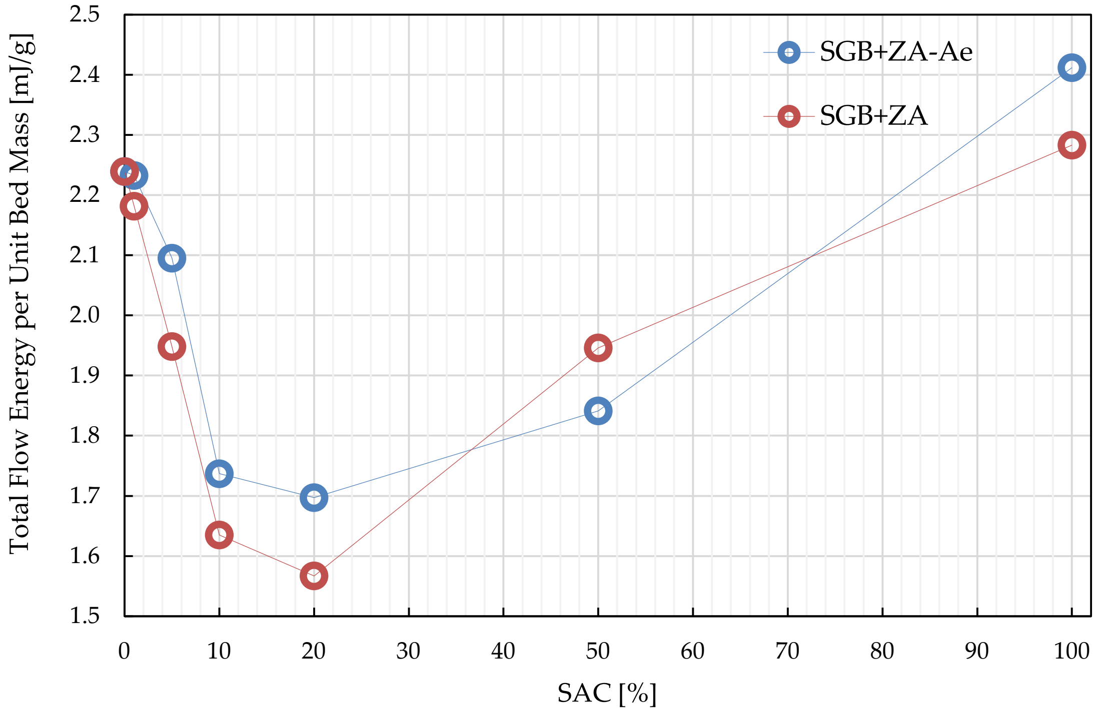

Figure 12. Total flow energy per unit bed mass of SGB coated with ZA and ZA-Ae at different SAC

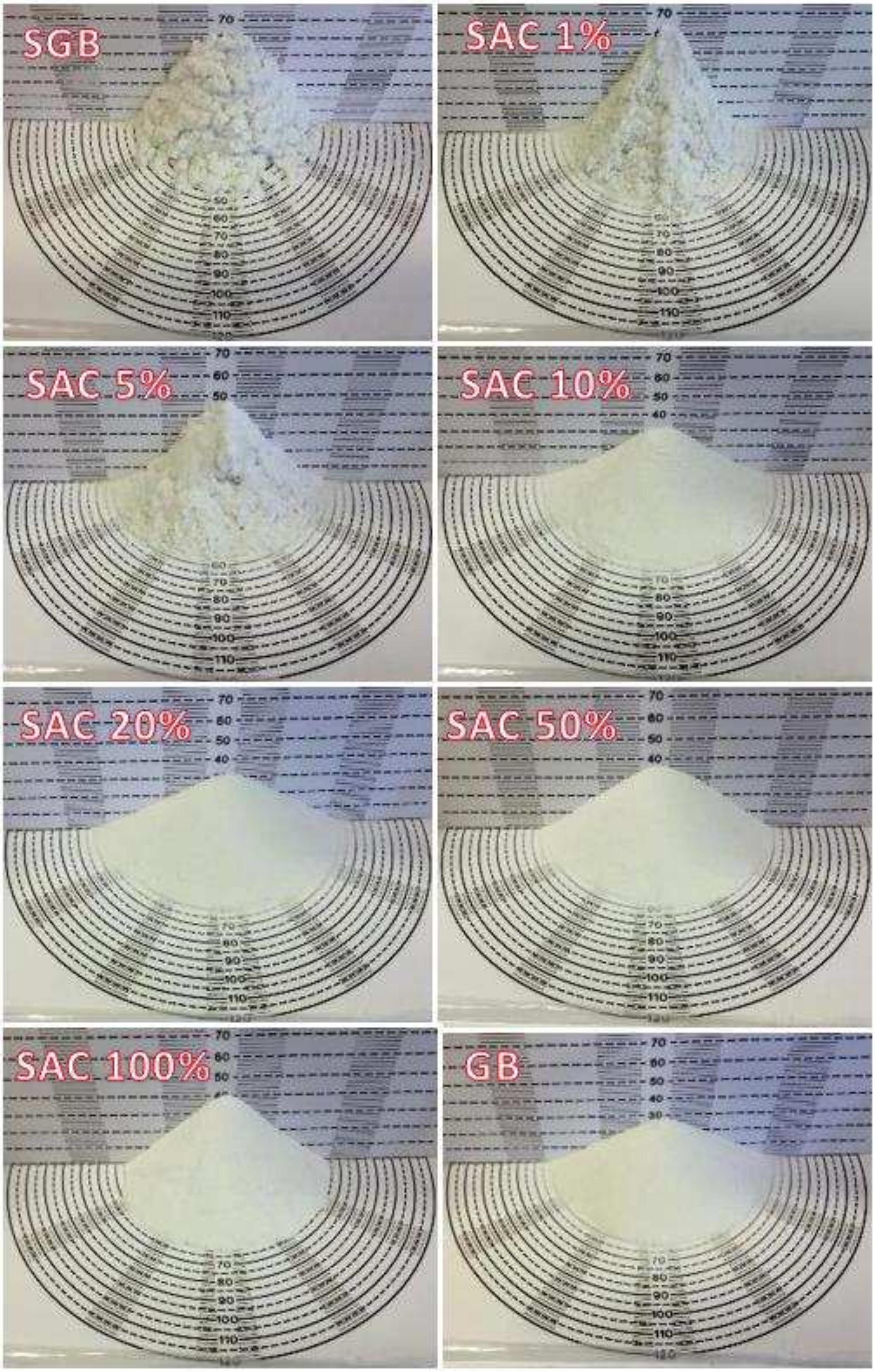

Figure 13. AoR of SGB, SGB+ZA-Ae at increasing SAC and GB, respectively

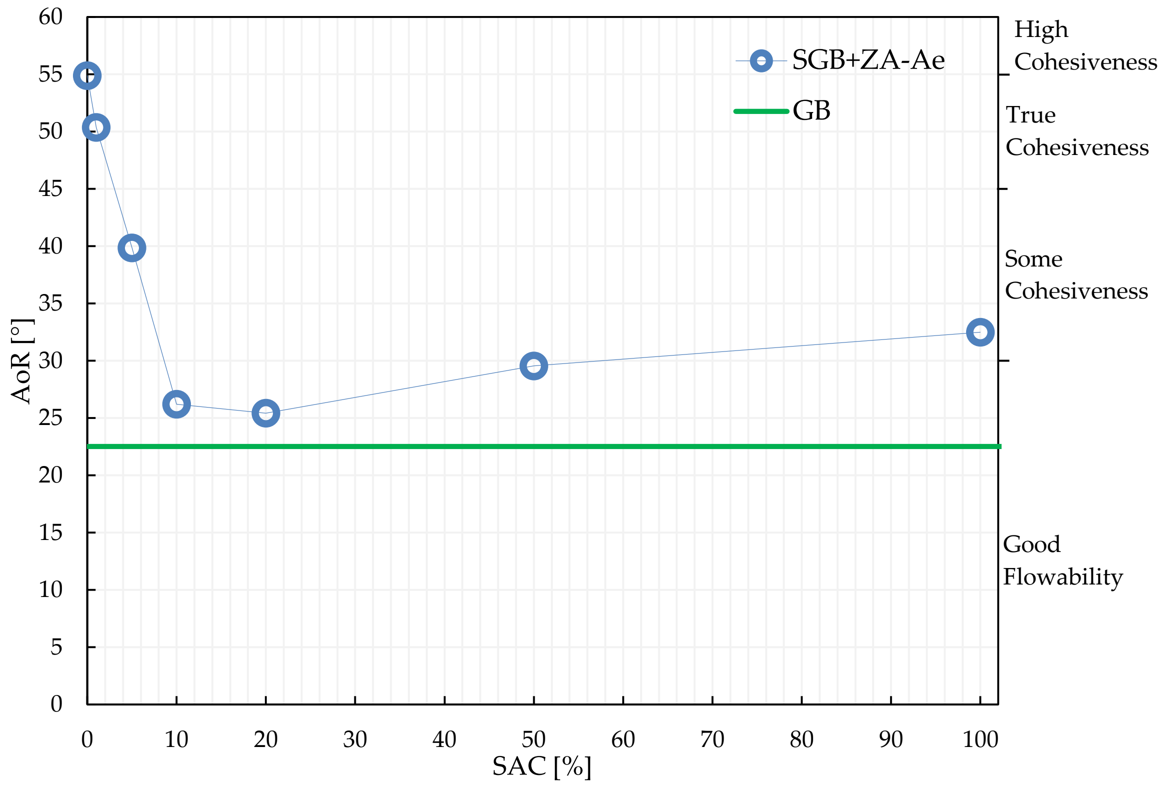

Figure 14. Angle of Repose of Silanised Glass Beads (SGB) coated with ZA-Ae at different SAC

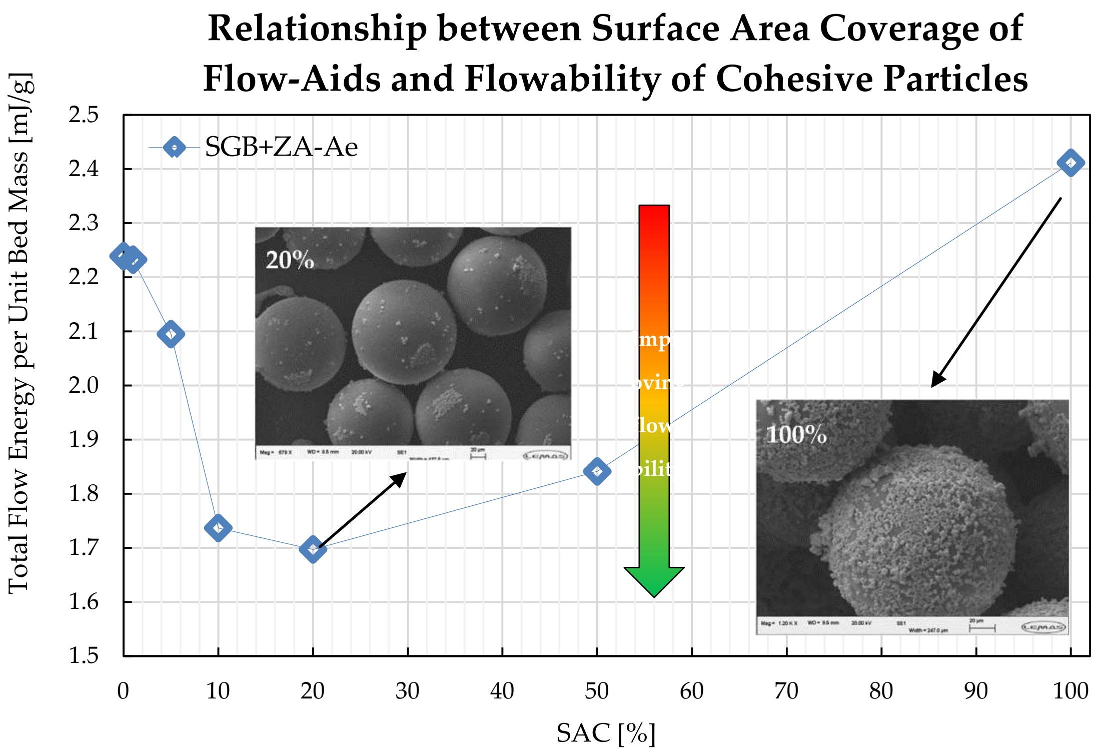

Graphical abstract

Highlights

- Sticky particles are made free flowing by the use of flow aids
- Surface area coverage is measured by image analysis
- Flowability is measured by three methods
- The optimum SAC for best flowability is around 20%